Thermodynamic curvature of soft-sphere fluids and solids

A. C. Brańka,[1,*] S. Pieprzyk,[1,†] and D. M. Heyes[2,‡]
[1]*Institute of Molecular Physics, Polish Academy of Sciences, M. Smoluchowskiego 17, 60-179 Poznań, Poland*
[2]*Department of Physics, Royal Holloway, University of London, Egham, Surrey TW20 0EX, United Kingdom*

(Received 31 October 2017; published 13 February 2018)

The influence of the strength of repulsion between particles on the thermodynamic curvature scalar R for the fluid and solid states is investigated for particles interacting with the inverse power (r^{-n}) potential, where r is the pair separation and $1/n$ is the softness. Exact results are obtained for R in certain limiting cases, and the R behavior determined for the systems in the fluid and solid phases. It is found that in such systems the thermodynamic curvature can be positive for very soft particles, negative for steeply repulsive (or large n) particles across almost the entire density range, and can change sign between negative and positive at a certain density. The relationship between R and the form of the interaction potential is more complex than previously suggested, and it may be that R is an indicator of the relative importance of energy and entropy contributions to the thermodynamic properties of the system.

DOI: 10.1103/PhysRevE.97.022119

I. INTRODUCTION

Riemannian geometry has attracted attention in the field of equilibrium thermodynamics [1–3]. In this approach the Riemannian curvature scalar, R, plays a central role. Its importance follows from the fact that in two dimensions all components of the Riemann tensor can be constructed using R. Consequently in two dimensions R provides complete information about the curvature at any particular point, and any thermodynamic curvature theory must be based on R [4]. In other words, the thermodynamic curvature at any state point characterized by R is independent of the coordinate system in which it is calculated. Therefore, R, as the geometric invariant in thermodynamics, is expected to contain information of intrinsic physical meaning. As will be discussed below, the R parameter defined in terms of derivatives of the free energy in the temperature-density plane can probe the underlying free energy landscape with key readily accessible thermodynamic quantities such as the heat capacity and bulk modulus. To extend our understanding of Riemannian geometry applied to thermodynamics it is important to analyze R for systems whose thermodynamic properties have been determined accurately and precisely.

Two main approaches have been used to investigate R. First, statistical mechanics can be applied for well defined model systems [4,5]. Second, a database of thermodynamic properties of various experimental liquids has been used [1,3]. R has been investigated for many systems [6], including the Bose and Fermi gas [7,8], Ising based models [9,10], van der Waals and Lennard-Jones liquids [4,5], as well as for over 120 real fluids, including water, carbon dioxide, hydrogen, and linear alkanes [1–3], taking data from thermodynamic databases.

The value of R across the phase diagram of various fluids might provide a new perspective on the thermodynamic properties and reveal insights into the underlying significance of their variation, which otherwise might be difficult to discern. The variations in R found in experimental systems, and presented in such diagrams, certainly coincide with well defined regimes in the phase diagram (e.g., near the critical point region, near the melting line, etc.). Therefore it might reasonably be expected that a link between R and some more basic thermodynamic or structural feature could eventually be found.

In spite of these previous studies, our knowledge of R and its meaning is still fairly incomplete. In particular its connection with the character of the microscopic interactions has not been convincingly established. Nevertheless, an emerging view is that the thermodynamic curvature scalar R may be a measure of the intermolecular interaction. The sign of R indicates whether the interaction or "effective" interaction is predominantly attractive ($R < 0$) or repulsive ($R > 0$) [6,11]. It has been proposed that $|R| \sim \xi^3$, where ξ is a correlation length, and therefore $|R|$ would be a measure of the size of mesoscopic organized structures [4,12]. Consequently, the locus of the maximum of $|R|$ has been used to describe the locus of the Widom line [13]. Also, as for the coexisting phases the correlation length is the same, calculation of $|R|$ can help in determining the vapor-liquid coexistence line [5,13]. Of particular interest is the $R = 0$ line which it has been suggested marks the transition from attractive to repulsive interaction dominated parts of the phase diagram. It has even been suggested that the $R = 0$ line could be connected to the Fisher-Widom line [14], which reflects a similar kind of transition. It is fair to say that the precise meaning of the $R = 0$ curve is still under debate.

To extend our understanding of the Riemannian geometry approach to thermodynamics, we require a systematic and precise analysis of the thermodynamic properties of a well-defined model particle system over many state points. A detailed analysis of the influence of the intermolecular

*branka@ifmpan.poznan.pl
†pieprzyk@ifmpan.poznan.pl
‡david.heyes@rhul.ac.uk

 ©2018 American Physical Society

attraction and repulsion terms on the curvature parameter R can then be better established. Only recently have systematic investigations of the dependence of R on the intermolecular interaction strength been performed. In those studies a tunable interaction going from the purely repulsive Weeks-Chandler-Andersen or WCA potential to the Lennard-Jones potential was used to monitor changes in R caused by increasing the contribution of the attraction part [15]. The results support the conjecture that the sign of R specifies whether the dominant part of the interparticle interaction is attractive ($R < 0$) or repulsive ($R > 0$).

Some work has been performed analyzing the effects of the strength of repulsion [16], but the results were inconclusive, presumably because the thermodynamic data was not precise enough. In this work a detailed investigation of R of the soft-sphere system in the fluid and solid phases has been performed, and the influence of strength of interparticle repulsion on R determined. The soft-sphere or inverse power potential (IP) was used, which is defined as $\phi(r) = \epsilon(\sigma/r)^n$, where r is the separation between two particles, σ is the particle diameter, ϵ sets the energy scale of the interparticle interaction, and $1/n$ is a parameter determining the potential softness. By varying n from very soft ($n \to 3$) to extremely hard ($n \to \infty$) this potential can be used to establish the consequences of softness on R. The study is limited to the softness range $n > 3$, because for $n \leqslant 3$ the volume integral of the potential diverges and the system becomes thermodynamically unstable.

There are at least two main reasons why the IP system can be considered to be the most suitable for investigating the influence of the repulsive part of any interaction on R. First, the IP system possesses the useful (even unique) property that its excess thermodynamic properties do not depend on the density and temperature separately but on a dimensionless combination of the two, a temperature-scaled packing fraction $\zeta = (\epsilon/k_BT)^{3/n}\rho\sigma^3\pi/6$, where $\rho = N/V$ is the number density, N is the number of particles in volume V, k_B Boltzmann's constant, and T the temperature. A direct consequence of this is that for a given n, the entire phase behavior on the (T,ρ) plane can be generated from evaluations along a single isotherm or isochore. A range of densities at constant reduced temperature $T^* = k_BT/\epsilon = 1$ is a popular practical choice.

Second, the IP system is, apart from the hard sphere (HS) case, one of the best characterised off-lattice systems. The thermodynamic properties of IP fluids have already been determined to a large extent [17–19], and the scale invariance of the IP potential allows us to obtain certain closed-form analytic expressions valid, for example, in the low and very high density limits. Some molecular dynamics (MD) simulations of these systems were carried out for this study to supplement the existing data.

In the Sec. II the curvature quantity, R, is expressed in a form suitable for its calculation for the IP system, and in determining informative limiting cases. In Sec. III the results for the IP fluid and solid phases are presented and discussed. A summary of the main conclusions is given in Sec. IV.

II. THEORY

The Riemannian curvature in (T,ρ) coordinates has the following form [4,5]:

$$R = \frac{1}{\sqrt{g}}\left[\frac{\partial}{\partial T}\left(\frac{1}{\sqrt{g}}\frac{\partial g_{\rho\rho}}{\partial T}\right) + \frac{\partial}{\partial \rho}\left(\frac{1}{\sqrt{g}}\frac{\partial g_{TT}}{\partial \rho}\right)\right], \quad (1)$$

where $g = g_{TT}g_{\rho\rho}$, $g_{TT} = -(1/T)\partial^2(\rho f)/\partial T^2$, $g_{\rho\rho} = (1/T)\partial^2(\rho f)/\partial\rho^2$, and f denotes the free energy per Boltzmann's constant and per particle. It can be shown that the quantity R, which has units of volume, can be expressed in terms of two basic measurable thermodynamic properties, the isochoric heat capacity $C_V = (\partial U/\partial T)_V$ and the isothermal bulk modulus $B_T = \rho(\partial P/\partial\rho)_T$ (i.e., the inverse of the system's compressibility), where U is the total energy and P is the pressure:

$$R^* = \frac{1}{B^*C^*}\left\{T\frac{\partial B^*}{\partial T}\left[1 - \frac{1}{2}T\frac{\partial \ln(B^*C^*)}{\partial T}\right] + T^2\frac{\partial^2 B^*}{\partial T^2} + \rho\frac{\partial C^*}{\partial\rho}\left[1 - \frac{1}{2}\rho\frac{\partial \ln(B^*C^*)}{\partial\rho}\right] + \rho^2\frac{\partial^2 C^*}{\partial\rho^2} - \frac{1}{2}\rho C^*\frac{\partial \ln(B^*/C^*)}{\partial\rho}\right\}, \quad (2)$$

where the asterisk indicates that the quantities are given in dimensionless form, i.e., $R^* = R\rho$, $C^* = C_V/k_BN$, and $B^* = B_T/\rho k_BT$. The above expression may have advantages for some physical systems as it enables characteristic features of R to be derived from available thermodynamic data. For any thermodynamically stable system the terms C^* and B^* are positive, so the sign of R will be determined by a combination of their first and second derivatives, i.e., the terms in curly brackets in Eq. (2). For different systems and thermodynamic conditions these derivatives may change in relative magnitude and sign, and therefore in general both positive and negative R could be obtained. It is noteworthy that when B^* and C^* are in fact constant, their derivatives are zero, which means that all terms in the curly brackets are zero, and consequently so is R. A well known example of this case is the ideal gas, where for any (T,ρ) the B^* and C^* are constant. The ideal gas case was discussed in Refs. [4,6,11], and this example gave rise to the interpretation that R is a measure of the interaction strength. Equation (2) indicates that $R^* = 0$ may be obtained in any situation when the expressions in the curly brackets sum up to zero, without necessarily both B^* and C^* being constant.

If C^* is nearly constant, R is determined practically only by B^* and its derivatives. This feature may be expected in systems where the short-ranged repulsive part dominates and ones that are close to being hard spheres as a limit. More detailed analysis of R requires an interparticle potential and the system's thermodynamic properties (i.e., C^* and B^* here). The IP system is a valuable model system in this respect, as the complexity of Eq. (2) can be reduced substantially and its thermodynamic properties accurately determined.

For the IP system, after some algebra, the formula in Eq. (2) reduces to the following:

$$R^* = \frac{\zeta}{B^*C^*}\left\{\frac{\partial(9B^*/n^2 + C^*)}{\partial\zeta}\left[1 - \frac{1}{2}\zeta\frac{\partial \ln(B^*C^*)}{\partial\zeta}\right] + \zeta\frac{\partial^2(9B^*/n^2 + C^*)}{\partial\zeta^2} - \frac{1}{2}C^*\frac{\partial \ln(B^*/C^*)}{\partial\zeta}\right\}. \tag{3}$$

Also, in this case the prime shorthand notation for derivatives can be used unambiguously and will be employed in what follows. Thus the above equation is, in more compact notation,

$$R^* = \frac{\zeta}{B^*C^*}\left\{(9B^*/n^2 + C^*)'\left[1 - \frac{1}{2}\zeta[\ln(B^*C^*)]'\right] + \zeta(9B^*/n^2 + C^*)'' - \frac{1}{2}C^*[\ln(B^*/C^*)]'\right\}. \tag{4}$$

Now using $C^* = 3/2 + 3Z/n - 9\zeta Z'/n^2$ and $B^* = 1 + Z + \zeta Z'$ [19], the relationship $9B^*/n^2 + C^* = 3/2 + 9/n^2 + (3/n + 9/n^2)Z$, where $Z = P/\rho k_B T - 1$ is the excess compressibility factor (ECF), can be obtained. Therefore, only Z, Z', and Z'' are involved in the above expression for R^*. The absence of terms involving the third derivative, Z''', is important, and a unique feature of the IP system. Note, that the presence of the second derivatives of B^* and C^* in Eq. (2) means that in the general case the third derivatives of P and U are required, which are normally difficult to obtain with sufficient accuracy, and can be a serious obstacle in the determination of R to sufficient precision. We verified that Eq. (4) is equivalent to those given by Ruppeiner in Eqs. (29)–(31) in Ref. [16].

Equation (4) can be rewritten as follows:

$$\begin{aligned} R^* &= \frac{\zeta}{B^*C^*}\left\{\left[(9B^*/n^2 + C^*)' + \zeta(9B^*/n^2 + C^*)'' + \frac{1}{2}(C^*)'\right] - \left[\frac{1}{2}\zeta(9B^*/n^2 + C^*)'[\ln(B^*C^*)]' + \frac{1}{2}C^*[\ln(B^*)]'\right]\right\} \\ &= R_1 - R_2, \end{aligned} \tag{5}$$

where $R^* = R_1 - R_2$ is the difference between two terms, $R_1 = \zeta[(9B^*/n^2 + C^*)' + \zeta(9B^*/n^2 + C^*)'' + (C^*)'/2]/(B^*C^*)$ and $R_2 = \zeta[\zeta(9B^*/n^2 + C^*)'[\ln(B^*C^*)]'/2 + C^*[\ln(B^*)]'/2]/(B^*C^*)$. Both terms are always positive (i.e., for any n and ζ), and therefore their relative magnitude alone determines the sign of $R(\zeta,n)$.

With Eq. (5), rigorous and useful results for several limiting cases can be obtained, of which five are identified below. The first is when $n \to \infty$, where the IP system manifests many properties the same as the hard sphere system [19]. Because for the HS system C^* is a constant, the term R_1 is zero, and therefore its thermodynamic curvature reduces to

$$R^*_{HS} = R^*(\zeta,\infty) = -\frac{\zeta(\ln B^*)'}{2B^*} = -\frac{\zeta(B^*)'}{2(B^*)^2}, \tag{6}$$

which is always negative. This is a significant result which is exact, and demonstrates that even at high fluid densities and in the crystal the thermodynamic curvature can be negative, i.e., $R < 0$. Moreover, significantly, this situation occurs for a system composed of particles interacting with an entirely repulsive potential.

The result obtained for the HS system gives rise to a question about its uniqueness: Is R also negative for any n range? At least a partial answer to this question may be obtained by considering steeply repulsive IP fluids (or SIP), which may be defined as those where n is approximately greater than about 70, and for which the thermodynamic behavior is so close to the HS over the entire fluid phase that a perturbation approach based on the HS fluid can be exploited [18,19]. The perturbation approach in this case can be based on an appropriate choice of an effective hard sphere diameter, σ^{ef}_{HS}. This can be used to define an effective packing fraction, $\zeta^{ef}_{HS}/\zeta = (\sigma^{ef}_{HS}/\sigma)^3$, which in turn is the solution of the equation $Z(\zeta,1/n) = Z_{HS}(\zeta^{ef}_{HS})$ [20,21]. Thus, knowing ζ^{ef}_{HS} we can obtain $Z(\zeta,1/n)$ of the SIP from the HS fluid formula. As has been shown the simplest solution for ζ^{ef}_{HS}, which well represents the SIP, is that by Barker and Henderson (BH) [22], which give $\zeta_{BH} = \zeta\Gamma(1 - 1/n)^3$ [18], where Γ is the Gamma function. A more complex analytic prescription could be used but the identity $\zeta^{ef}_{HS} = \zeta_{BH}$ is sufficiently accurate for the present purpose. With ζ_{BH} the SIP ECF can be represented by $Z = Z_{HS} + \varepsilon\zeta Z'_{HS} + O(\varepsilon^2)$, where $\varepsilon = \Gamma(1 - 1/n)^3 - 1 \sim 1/n$. Using this representation of Z, it can be shown that the thermodynamic curvature of the SIP has the form $R^*(\zeta,1/n) = R^*_{HS} + \varepsilon F + O(\varepsilon^2)$, where F is a function of Z_{HS} and its derivatives. Importantly, this function is positive, which means that for SIP fluids $R^* > R^*_{HS}$. Thus, on increasing n, the R^* continuously approaches R^*_{HS} from above, which means that the HS system is the lower bound for the SIP fluids and indicates that there may exist a range of n for which $R^*(\zeta,1/n) < 0$.

The third rigorous case is in the low density limit, where Eq. (5) yields

$$R^*(\zeta \to 0,n) = -\left(1 - \frac{3}{n} - \frac{3}{n^2}\right)b_2(n)\zeta, \tag{7}$$

and $b_2(n) = 4\Gamma(1 - 3/n)$ is the second virial coefficient of the IP system. This result indicates that at very low ζ the thermodynamic curvature can be negative or positive, depending on the value of the system's softness parameter, $1/n$. The initial slope of $R^*(\zeta)$ changes sign at a particular value of n or $n = n_0 = (3 + \sqrt{21})/2 \approx 3.7913$ for which the term in parentheses in Eq. (7) becomes zero. This is a significant result as it indicates that for n greater than a certain value, n_0, that is, for most of the IP systems considered typically, it is expected that R^* changes sign from negative to positive at a certain packing fraction value, $\zeta = \zeta_0$.

The fourth important limiting case is in the very soft-sphere limit, i.e., $n \to 3$. In this limit the ECF is determined mainly by the second virial coefficent, and as was argued in Ref. [19,23] the ECF may be represented in the fluid phase by the simple

formula, $Z(\zeta,n \to 3) \to b_2(n)\zeta + \gamma\zeta^{\alpha}$, where $\alpha \approx 0.5$ and $\gamma \approx 1.5$. Because $b_2(n \to 3) \to \infty$ both Z and Z' also tend to ∞. However, many thermodynamic properties that are combinations of these two quantities have a finite value in the $n \to 3$ limit, e.g., $C^* \to 1.5 + (1-\alpha)\gamma\zeta^{\alpha}$ [19]. With this ECF the thermodynamic curvature is always positive as $R_1 > R_2$ for any $\zeta > 0$, and

$$R^*(\zeta > 0, n \to 3) \to \frac{4+\sqrt{\zeta}}{3(2+\sqrt{\zeta})^2}. \tag{8}$$

Taking into account these additional results for the low density limit given in Eq. (7), it is reasonable to expect that the thermodynamic curvature of very soft ($3 < n < n_0$) inverse power fluids is always positive, or $R^* > 0$.

For the fifth case, which is concerned with the solid phase, it is known that the IP fluid on increasing density transforms into a crystal structure which is FCC for $n > n_t$ and BCC for $n < n_t$, where n_t is estimated to be about 6 [17,24]. For the static perfect crystalline structure the total internal energy per particle, $u = U/Nk_BT$ can be readily computed, and from this the ECF becomes $Z = nu/3$. It can be verified that the ECF of the perfect cubic structure (FCC and BCC) is well represented by the simple formula $Z_S = a_n\zeta^{n/3} + n/2$, where a_n is an n-dependent constant. This is consistent with $Z'_S = nZ_S/3\zeta$ and $Z''_S = n(n-3)Z_S/9\zeta^2$, which gives $B^* = a_n\zeta^{n/3}(n/3+1) + 1 + n/2$, and $C^* = 3$ which is in agreement with the Dulong-Petit law for heat capacity.

These B^* and C^* substituted in Eq. (5) give a thermodynamic curvature which tends to $1/6$ for large ζ. This means that all IP solids have the same limiting R^* value, irrespective of the interaction softness. Therefore, the R^* quantity captures a fundamental difference between the IP and HS potentials. The HS potential has at the close packing density ($\zeta_{cp} = \sqrt{2}\pi/6 = 0.7405$) the limit $R^* \to 0$. In contrast, the soft-sphere crystal can be compressed without any bounds, and in this case $R^*(\zeta \to \infty, n) \to 1/6$. Thus, the ζ limits for $R^*(1/n \to 0)$ and $R^*(1/n = 0)$ are different. For arbitrarily large n there exists a value of ζ at which R^* changes sign from negative to positive, and only for the HS crystal does R^* remain always nonpositive. Note also that, in the high density limit, $R = R^*/\rho$ tends to zero, in both cases, but for any IP crystal from above (the 0^+ limit) and for the HS system from below (the 0^- limit).

From the above analysis of Eq. (5), it may be observed that by merely changing the softness of the repulsive particle, three qualitatively different types of behavior in R can be obtained: only negative, negative and positive, and only positive. We note that for purely repulsive particles, for most of the density range (even in solid phase), R is negative. We consider this to be a significant result as in the literature a repulsive interaction has been associated with a positive R. Indeed, it is difficult to interpret $R < 0$ for nearly HS particles as being "effectively attractive" (particularly for a fluid).

III. RESULTS AND DISCUSSION

To obtain sufficiently accurate results for R, the data for the ECF of the IP systems from Refs. [19,23] and for the hard sphere fluid from Ref. [25] were used, and additional molecular dynamics simulations for these systems were carried out. The new calculations were performed for steeply repulsive potential fluids with exponents, $n = 36$, 72, 88, and 144, and for very soft IP particles using $n = 4$ and 5. Long simulations were necessary to obtain sufficient accuracy for Z at high packing fractions. For the crystalline (FCC) phase the calculations were performed for $n = 12$, 72, and 144 IP systems and for hard spheres. The simulations were carried out mostly with $N = 4000$ particles. The equations of motion were integrated with the leap-frog Verlet algorithm with a time step of $dt = 0.001$ for $n > 12$ and $dt = 0.005$ for $n < 12$. The interaction truncation distance, r_c, was where the potential was 0.0001. The averages were calculated from well-equilibrated simulations of length 4×10^5 time steps. The accuracy of the resultant Z was estimated to be better than $\leqslant 0.2\%$. The hard sphere data were generated with the DYNAMO code [26] for $N = 131\,072$ particles with 10^9 collisions.

A. Inverse power, IP fluid

Figure 1 shows the calculated thermodynamic curvature of the IP fluids for a number of representative n values which cover the entire range of softness, i.e., $0 \leqslant 1/n < 1/3$. In the figure the different kinds of limiting behavior discussed in Sec. II are clearly visible. That is, the HS fluids bound the IP system from below, and R^* for SIP fluids can be negative especially for large n and density. For soft particle fluids R^* is predominantly positive. On increasing the interaction softness, three different types of behavior are revealed. If n_f is a particular value of n, (a) for $0 \leqslant 1/n < 1/n_f$ the thermodynamic curvature is negative, (b) for $1/n_f < 1/n < 1/n_0$ the curvature, R^* changes sign at a certain packing fraction, $\zeta_0(n)$, and (c) for $1/n_0 < 1/n < 1/3$ the thermodynamic curvature is positive. Also, $R^*(n \to 3)$ is the upper bound for the IP fluids (the bold green line in the figure) at all densities.

It was found that, by applying the BH perturbation approach to the SIP fluids near freezing using the HS equation by Kolafa, Labík, and Malijevský [25] (or any other accurate formula for the hard sphere compressibility factor), it is when $n_f = 88$ that

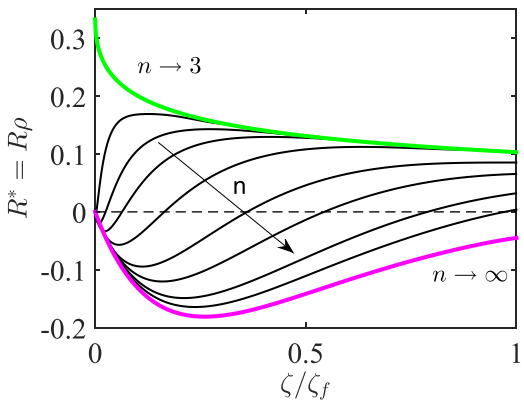

FIG. 1. The thermodynamic curvature of IP fluids. The lines from bottom to top are for the HS fluid (magenta bold line) and $n = 72,36,18,12,8,6,5,4$ (black lines). The top green bold line represents the limiting formula in Eq. (8) for $R^*(\zeta > 0, n \to 3)$. The freezing point packing fractions ζ_f are obtained from Ref. [27]: 0.487,0.492,0.531,0.610,0.825,1.22,1.73,2.98 for the corresponding n values. In the calculations the MD simulation data and the ECF for the hard sphere fluid from Ref. [25] were used.

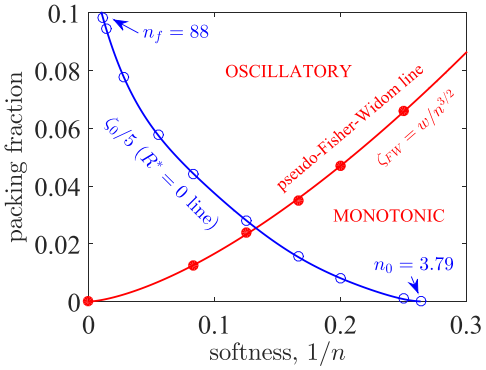

FIG. 2. The packing fraction value, ζ_0, at which the thermodynamic curvature $R^* = 0$. The open symbols are from the curves in Fig. 1, the end points are $\zeta_0(n_f) = \zeta_f(n = 88) = 0.492$ and $\zeta_0(n_0) = 0$, and the solid (blue) line is a polynomial fit (note the function is divided by 5 on the figure). The bold solid (red) line represents the pseudo-Fisher-Widom line for the IP fluids ($w = 0.525$). It is obtained as a fit to $\zeta_{FW}(1/n)$ (solid red circles) determined from the MD data and which represent a crossover from oscillatory to monotonic behavior of the radial distribution function.

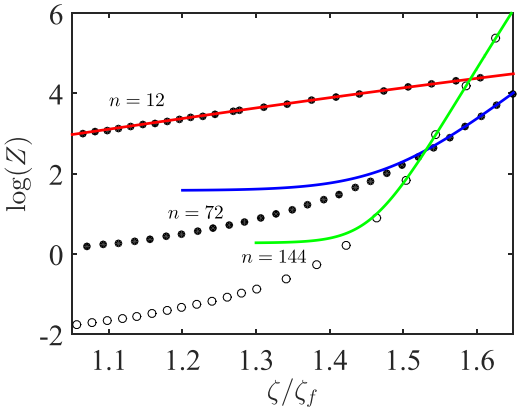

FIG. 3. The ECF of IP solids vs ζ/ζ_f shown on a log-linear scale (note log is the natural logarithm). The symbols are the MD results for $n = 12, 72$, and 144 IP systems. The continuous curves represent $Z = a_n\zeta^{n/3} + n/2$; $\log(a_{12}) = 4.3908$, $\log(a_{72}) = 12.1808$, $\log(a_{144}) = 20.0848$ for the cubic crystal. On the figure, the $\log(Z)$ for $n = 72$ and 144 are shifted down by 2 and 4, respectively.

$R^* = 0$ at the freezing packing fraction. Thus for all fluids with $n > 88$ the corresponding R is negative near freezing.

The softness (i.e., $1/n$) dependence of the packing fraction at which $R^* = 0$ or ζ_0 is shown in Fig. 2, which shows that it is a monotonically decreasing function which starts at $n = n_f$ and terminates at $n = n_0$. Possible relationships between R and various physical properties have been the subject of debate in the literature, one suggestion being that the $R^* = 0$ line may be linked to or even coincide with the so-called Fisher-Widom (FW) line [12]. The FW is a line in the density-pressure plane along which a change from monotonic to damped oscillatory decay in the radial distribution function (RDF) takes place [14]. This is interpreted as being a crossover from domination by the attractive to the repulsive interaction, and if a similar interpretation for the $R = 0$ line is made, it might be expected that the two lines are fundamentally connected. In the case of fluids with short-ranged interactions, the FW line can be determined by the conventional pole structure approach [28–30]. In the case of the inverse power fluid the ultimate (large r) decay is algebraic, as is the potential itself. Consequently there is a qualitative difference in the asymptotic behavior of the RDF in fluids composed of particles with finite ranged or exponentially decaying potentials and fluids composed of particles with long-ranged interactions. However, in the last case instead of the FW line the pseudo-FW line can be defined. The pseudo-FW line defines the crossover from pseudoexponential to damped oscillatory contributions to the RDF, and follows from the existence of a complex (pseudo-exponential) pole positioned very close to the imaginary axis [31,32]. Thus the term FW line for the IP systems is to be understood as the pseudo-FW line.

In the case of the inverse power fluid, due to the scaling properties of the IP interaction, we have points (one for each value of n) instead of lines. Just as the $R = 0$ line in the density-temperature plane is represented by a single ζ_0 point, we have a FW point for the FW line. A number of FW points or ζ_{FW} have been estimated for several different softness values using the pole structure method [31,32]. It was found that they can be represented well by the simple algebraic formula, $\zeta_{FW} = w/n^{3/2}$, where $w = 0.525$. It can be seen in Fig. 2 that in the case of the IP fluid it is not easy to find any simple relationship between the zero R and FW lines. In fact the trends are to a large extent opposite, as ζ_0 decreases and ζ_{FW} increases with increasing $1/n$.

B. Inverse power, IP solid

As mentioned above, at a certain packing fraction, the IP system freezes into a crystalline solid. It is expected that in the HS solid the thermodynamic curvature remains negative up to the close packing density and that for any $1/n > 0$, on increasing ζ, R^* converges towards $1/6$ (i.e., to a single positive value). The calculations for the HS solid were performed with the DYNAMO program [26] for a very large system composed of $N = 10^5$ particles. Such large systems were used to establish the ECF with an accuracy of 10^{-5}, which in turn allowed us to assess the performance of the Speedy formula [33],

$$Z = \frac{3\zeta_{cp}}{\zeta_{cp} - \zeta} - \frac{a(\zeta - b\zeta_{cp})}{(\zeta - c\zeta_{cp})} - 1, \tag{9}$$

where $a = 0.5921$, $b = 0.7072$, and $c = 0.601$. We have found that the Speedy formula represents the HS solid structure for all packing fractions greater than the melting $\zeta_m = 0.545$ with an accuracy better than 10^{-3}. The Speedy formula yields practically the same R^* as that obtained directly from the current MD data. It is noteworthy that the very good agreement between the MD data and the Speedy formula indicates that the limiting form of the ECF is not a logarithmic divergence [16], but $Z(\zeta \to \zeta_{cp}) \sim 1/(1 - \zeta/\zeta_{cp})$.

The density dependence of $\log(Z)$ given in Fig. 3 for three different softness values shows that at a certain value of ζ (corresponding to the situation when the soft-spheres start to overlap substantially or r becomes less than σ) the excess compressibility factor starts to be represented very well by the static lattice approximation (the continuous line on the figure). The static lattice approximation predicts that on increasing

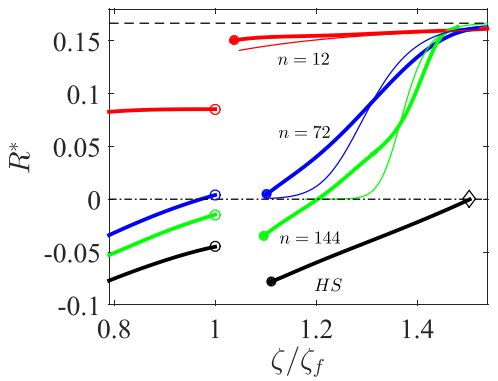

FIG. 4. The thermodynamic curvature scalar, R^*, of the IP potential solids vs ζ/ζ_f. The bold lines from bottom to top represent the HS and $n = 144$, 72, and 12 IP systems obtained from MD results. The R values from the Speedy formula in Eq. (9) are superimposed on the figure as a solid line for the HS systems. The symbols denote the freezing (open circles) and melting (solid dots) packing fractions taken from Ref. [27]. The thin lines mark out the static model values. The diamond terminating the HS line in the solid phase is at the HS close packed density. The dashed line marks out the limiting 1/6 value.

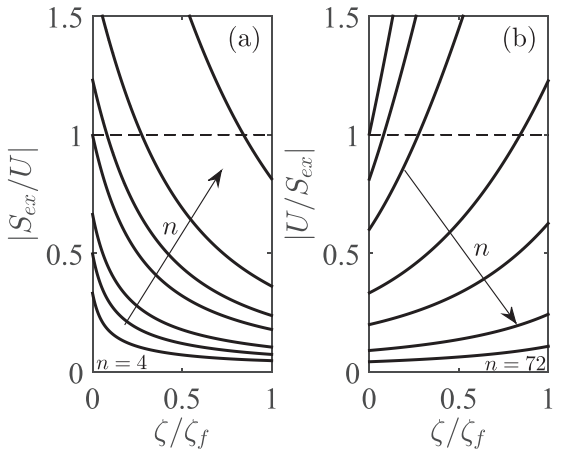

FIG. 5. Relative contribution of the total energy and excess entropy in the IP fluid with different n. The ratio S_{ex}/U on the left-hand frame (a) shows that for $n < 4$ the energetic contribution becomes order of magnitude larger than the entropic one. For U/S_{ex} on the right-hand frame (b), it may be seen that for $n > 72$ the energetic contribution is an order of magnitude smaller than the entropic one.

density all IP solids must tend towards a positive value of $R^* = 1/6$, which implies that R^* of dense IP solids is positive and can be represented well (at least for $\zeta > 1.5\zeta_f$) in analytic form calculated from the static Z_S calculation.

The R^* values for the solid phase and the transition region are shown in Fig. 4. The fluid-solid coexistence line for the soft-sphere fluid as a function of n was determined by Agrawal and Kofke [27] and the coexistence fluid and solid packing fractions, ζ_f and ζ_m, respectively, were taken from that work.

In the case of the HS system the thermodynamic curvature R^* increases almost linearly from about -0.09 at ζ_m to the limiting zero value at ζ_{cp}, the maximum packing density. Also note that $R^*_{HS}(\zeta_f) > R^*_{HS}(\zeta_m)$, and that in general $R^*(\zeta_f,n) \neq R^*(\zeta_m,n)$, which implies that the thermodynamic curvature is not a property that can be used to identify the location of the freezing transition. Also note that for $R^*(\zeta_f) < 0$ we have $R^*(\zeta_f) > R^*(\zeta_m)$, and for $R^*(\zeta_f) > 0$ the inverse relation occurs, i.e., $R^*(\zeta_f) < R^*(\zeta_m)$. As may be seen, for the solid IP systems (where $n = 12$, 72, and 144), R^* increases monotonically towards a limiting value of 1/6. As discussed above, at high densities R^* is well represented by the static approximation (the continuous line on the figure). In the case of $n = 12$ (and for softer interactions) the static approximation works well over most of the solid phase, and the R value depends weakly on ζ as the function $R^*(\zeta)$ becomes quite flat. Note the results for $n = 144$ indicate clearly that, for large n, the crossing $R^* = 0$ value is located in the solid phase. Therefore it can be concluded that there are solids composed of purely repulsive particles for which the scalar curvature is negative for a range of densities.

IV. CONCLUSIONS

The influence of softness or the strength of repulsion between particles on the thermodynamic curvature scalar R has been investigated. The soft repulsive sphere or inverse power (IP) potential with variable exponent was used for the system over the entire stable range. It was shown that R for the hard sphere system is negative and constitutes a lower bound for all inverse power systems. Also R^* of the IP systems in the solid phase must tend to a common limiting value at high density.

By changing the interaction softness a qualitative change in R^* behavior takes place. For very soft systems R is always positive, and on decreasing softness R changes sign from being negative to positive at a certain packing fraction. For the steeply repulsive soft inverse power systems the behavior is (apart from in the very dense solid region) like that of the hard sphere, i.e., $R < 0$.

The results obtained clearly indicate that a purely repulsive interaction between particles can give rise to a negative as well as an "expected" (based on previous literature [6,11]) positive R. Moreover, apart from very soft particle systems, the negative sign seems to be a characteristic feature at low densities. For steeply repulsive particles any interpretation in terms of an effective attractive causing clustering in the low density region seems to us to be questionable. The results obtained broaden the spectrum of possible interpretations of R, rather than just whether the attractive or repulsive terms dominate. Certainly further study of the relationship between the sign and magnitude of R and the structural properties of the inverse power potential system could well prove informative.

Also, the IP results may suggest an interpretation of R as an indicator of the energy-to-entropy balance in the system. Figure 5 shows that the ratio entropy/energy (S_{ex}/U) is more than 10 for $n > 72$ and less than 0.1 for $n < 4$ for all of the fluid phase. In other words, the energetic contribution is an order of magnitude larger (lower) than the entropic one for $n < 4$ (for $n > 72$). Therefore, Fig. 5 demonstrates that for a very soft system with a long range repulsion (characterized by $R > 0$) the energetic part dominates, and for the steeply repulsive cases (characterized by $R < 0$) entropy dominates. It would be interesting to explore further the observed relationship for

some colloidal systems which are driven purely by entropy (e.g., see Refs. [34,35]).

To conclude, our results show that the dependence of R on the details of the interaction potential and the physical state of the system can be more complex than has hitherto been suggested.

ACKNOWLEDGMENTS

D.M.H. would like to thank Dr. T. Crane (Department of Physics, Royal Holloway, University of London) for helpful software support. Some of the calculations were performed at the Poznań Supercomputing and Networking Center (PCSS).

[1] G. Ruppeiner, N. Dyjack, A. McAloon, and J. Stoops, J. Chem. Phys. **146**, 224501 (2017).
[2] H.-O. May, P. Mausbach, and G. Ruppeiner, Phys. Rev. E **91**, 032141 (2015).
[3] G. Ruppeiner, P. Mausbach, and H.-O. May, Phys. Lett. A **379**, 646 (2015).
[4] G. Ruppeiner, Rev. Mod. Phys. **67**, 605 (1995); **68**, 313(E) (1996).
[5] H.-O. May and P. Mausbach, Phys. Rev. E **85**, 031201 (2012).
[6] G. Ruppeiner, Am. J. Phys. **78**, 1170 (2010).
[7] H. Janyszek and R. Mrugała, J. Phys. A: Math. Gen. **23**, 467 (1990).
[8] M. R. Ubriaco, Physica A **392**, 4868 (2013).
[9] W. Janke, D. A. Johnston, and R. P. K. C. Malmini, Phys. Rev. E **66**, 056119 (2002).
[10] W. Janke, D. A. Johnston, and R. Kenna, Phys. Rev. E **67**, 046106 (2003).
[11] G. Ruppeiner, J. Low Temp. Phys. **185**, 246 (2016).
[12] G. Ruppeiner, Phys. Rev. E **86**, 021130 (2012).
[13] G. Ruppeiner, A. Sahay, T. Sarkar, and G. Sengupta, Phys. Rev. E **86**, 052103 (2012).
[14] M. E. Fisher and B. Widom, J. Chem. Phys. **50**, 3756 (1969).
[15] H.-O. May, P. Mausbach, and G. Ruppeiner, Phys. Rev. E **88**, 032123 (2013).
[16] G. Ruppeiner, Phys. Rev. E **72**, 016120 (2005).
[17] S. Prestipino, F. Saija, and P. V. Giaquinta, J. Chem. Phys. **123**, 144110 (2005).
[18] A. C. Brańka and D. M. Heyes, Phys. Rev. E **74**, 031202 (2006).
[19] S. Pieprzyk, D. M. Heyes, and A. C. Brańka, Phys. Rev. E **90**, 012106 (2014).
[20] P. Egelstaff, *An Introduction to the Liquid State* (Clarendon, Oxford, 1992).
[21] F. del Río, Mol. Phys. **76**, 29 (1992).
[22] J. A. Barker and D. Henderson, J. Chem. Phys. **47**, 4714 (1967).
[23] D. M. Heyes, S. M. Clarke, and A. C. Brańka, J. Chem. Phys. **131**, 204506 (2009).
[24] W. G. Hoover, S. G. Gray, and K. W. Johnson, J. Chem. Phys. **55**, 1128 (1971).
[25] J. Kolafa, S. Labík, and A. Malijevský, Phys. Chem. Chem. Phys. **6**, 2335 (2004).
[26] M. N. Bannerman, R. Sargant, and L. Lue, J. Comput. Chem. **32**, 3329 (2011).
[27] R. Agrawal and D. A. Kofke, Mol. Phys. **85**, 23 (1995).
[28] R. J. F. Leote de Carvalho, R. Evans, D. C. Hoyle, and J. R. Henderson, J. Phys.: Condens. Matter **6**, 9275 (1994).
[29] M. Dijkstra and R. Evans, J. Chem. Phys. **112**, 1449 (2000).
[30] J. P. Hansen and I. R. McDonald, *Theory of Simple Liquids: With Applications of Soft Matter*, 4th ed. (Academic, New York, 2013).
[31] R. Evans and J. R. Henderson, J. Phys.: Condens. Matter **21**, 474220 (2009).
[32] A. C. Brańka and D. M. Heyes, J. Chem. Phys. **134**, 064115 (2011).
[33] R. J. Speedy, J. Phys.: Condens. Matter **10**, 4387 (1998).
[34] F. Smallenburg, L. Leibler, and F. Sciortino, Phys. Rev. Lett. **111**, 188002 (2013).
[35] F. Smallenburg and F. Sciortino, Nat. Phys. **9**, 554 (2013).